

Highly Cooperative Ca^{2+} Elevations in Response to $\text{Ins}(1, 4, 5)\text{P}_3$ Microperfusion Through a Patch-Clamp Pipette

J. Schrenzel,* N. Demaurex,* M. Foti,* C. Van Delden,* J. Jacquet,† G. Mayr,§ D. P. Lew,§ and K. H. Krause*

*Infectious Diseases Division, University Hospital and †SICMU, Geneva, 1211 Geneva 14, Switzerland, and §University of Hamburg, Hamburg, Germany

ABSTRACT To study the initial kinetics of $\text{Ins}(1, 4, 5)\text{P}_3$ -induced $[\text{Ca}^{2+}]_i$ elevations with a high time resolution and to avoid the problem of cell-to-cell heterogeneity, we have used the combined patch-clamp/microfluorimetry technique. The mathematical description of the microperfusion of $\text{Ins}(1, 4, 5)\text{P}_3$ and the subsequent Ca^{2+} release consists of a monoexponential decay (cytosolic $\text{Ins}(1, 4, 5)\text{P}_3$ concentration) and a Hill equation ($\text{Ins}(1, 4, 5)\text{P}_3$ dose-response curve). Two additional Hill equations and an integration were necessary to include a putative dependence of $\text{Ins}(1, 4, 5)\text{P}_3$ -induced Ca^{2+} release on $[\text{Ca}^{2+}]_i$. Best-fitting analysis assuming $[\text{Ca}^{2+}]_i$ -independent Ca^{2+} release yielded Hill coefficients between 4 and 12. The high cooperativity was also observed with the poorly metabolizable analog $\text{Ins}(2, 4, 5)\text{P}_3$ and was independent of extracellular $[\text{Ca}^{2+}]_i$. Best-fitting analysis including a positive $[\text{Ca}^{2+}]_i$ feedback suggested a cooperativity on the level of $\text{Ins}(1, 4, 5)\text{P}_3$ -induced channel opening ($n = 2$) and an enhancement of $\text{Ins}(1, 4, 5)\text{P}_3$ -induced Ca^{2+} release by $[\text{Ca}^{2+}]_i$. In summary, the onset kinetics of $\text{Ins}(1, 4, 5)\text{P}_3$ -induced $[\text{Ca}^{2+}]_i$ elevations in single HL-60 granulocytes showed a very high cooperativity, presumably because of a cooperativity on the level of channel opening and a positive Ca^{2+} feedback, but not because of Ca^{2+} influx or $\text{Ins}(1, 4, 5)\text{P}_3$ metabolism. This high cooperativity, acting in concert with negative feedback mechanisms, might play an important role in the fine-tuning of the cellular Ca^{2+} signal.

INTRODUCTION

Since the demonstration of receptor-mediated phospholipase C activation, the demonstration of Ca^{2+} release in response to $\text{Ins}(1, 4, 5)\text{P}_3$, and the purification and cloning of $\text{Ins}(1, 4, 5)\text{P}_3$ -sensitive Ca^{2+} release channels, inositol phosphate signaling has been rapidly accepted as an important cellular second messenger system (for a review see Berridge, 1993). However, because of refinements in the technique of $[\text{Ca}^{2+}]_i$ measurements, the simple view of a proportional increase in Ca^{2+} store permeability in response to increases in the intracellular $\text{Ins}(1, 4, 5)\text{P}_3$ concentration has quickly been challenged. Phenomena such as “ Ca^{2+} oscillations,” “ Ca^{2+} waves,” “lag times followed by abrupt Ca^{2+} increases,” “all-or-nothing Ca^{2+} mobilization,” and “quantal Ca^{2+} release” (e.g., Oldershaw et al., 1991; Berridge, 1993; Bootman et al., 1992) are found in virtually all cell types and cannot be explained by a simple proportional model. Accordingly, a variety of positive and negative feedback mechanisms have been postulated and experimentally demonstrated.

The concept of cooperativity of $\text{Ins}(1, 4, 5)\text{P}_3$ -induced Ca^{2+} release plays a key role in many models of $[\text{Ca}^{2+}]_i$ homeostasis. Indeed, two studies by Meyer et al. (1988, 1990), using stopped-flow measurements with high time resolution, suggested a high cooperativity of the early kinetics of $\text{Ins}(1, 4, 5)\text{P}_3$ -induced Ca^{2+} release ($n > 3$). However, some studies investigating $\text{Ins}(1, 4, 5)\text{P}_3$ -induced Ca^{2+} release found no cooperativity (Bezprozvanny et al., 1991; Finch et al., 1991).

To study the cooperativity of $\text{Ins}(1, 4, 5)\text{P}_3$ -induced $[\text{Ca}^{2+}]_i$ elevations in single HL-60 granulocytes with a high time resolution, we have used the combined patch-clamp/microfluorimetry technique. The comparison of a mathematical model with the experimental results suggests a high cooperativity of the onset of the $\text{Ins}(1, 4, 5)\text{P}_3$ response, independently of $\text{Ins}(1, 4, 5)\text{P}_3$ metabolism and Ca^{2+} influx.

MATERIALS AND METHODS

Culture of HL-60 granulocytes

The human promyelocytic cell line HL-60 was cultured in the tissue culture medium RPMI 1640 supplemented with 10% fetal calf serum, penicillin (5 units ml^{-1}), streptomycin (50 $\mu\text{g ml}^{-1}$), and L-glutamine (2 mM). The cells were passaged two times per week and differentiated by adding dimethylsulfoxide (DMSO; final concentration 1.3% v/v) to the cell suspension 7 days before experiments. The DMSO-differentiated cells display a neutrophil granulocyte phenotype, as previously discussed (Varnai et al., 1993); they will be referred to as HL-60 granulocytes.

Whole-cell patch-clamp technique and microperfusion of inositol phosphates

We used the patch-clamp whole-cell configuration to voltage-clamp cells and to microperfuse inositol phosphates (Hamill et al., 1981). Patch-clamp

Received for publication 30 December 1994 and in final form 8 September 1995.

Address reprint requests to Dr. Jacques Schrenzel, Infectious Diseases Division, University Hospital, 1211 Geneva 14, Switzerland. Tel: (41) 22/3729815; Fax: (41) 22/3729830; E-mail: schrenze@dminov1.hcuge.ch.

Abbreviations used in the Appendix: InsP_3 response, InsP_3 -induced Ca^{2+} release; $[i]_i$, cytosolic InsP_3 concentration (μM); $[i]_p$, InsP_3 concentration in the patch pipette (μM); τ , time constant for InsP_3 diffusion from the patch pipette into the cytoplasm (s); K_d , apparent constant of dissociation for InsP_3 binding (μM); EC_{50} , InsP_3 concentration eliciting half-maximal Ca^{2+} release (μM); f , InsP_3 concentration expressed as a fraction of the EC_{50} ; n , Hill coefficient.

© 1995 by the Biophysical Society

0006-3495/95/12/2378/14 \$2.00

electrodes were pulled from borosilicate glass (external diameter 1.2 mm; Mecanex, Nyon, Switzerland) using a BB-CH-PC puller (Mecanex). Pipettes were filled with (in mM): KCl 140; NaCl 5; MgCl₂ 1; EGTA 0.2; HEPES 20; and indo-1 free acid 0.01 (pH 7.2) and InsP₃ isomers to be microperfused were added in the pipette solution before the experiment. Under these conditions, [Ca²⁺]_i in the pipette was 120 nM, as measured using a Ca²⁺-sensitive electrode. Pipette resistances varied between 5 and 15 MΩ, and seal resistances between 5 and 50 GΩ. After achieving the seal, a burst of suction caused the appearance of capacitive currents, indicating that the whole-cell configuration had been obtained. Patch-clamp recordings were made using a List EPC-7 amplifier (List Medical, Darmstadt, Germany) in the voltage-clamp mode. The holding voltage was clamped at -60 mV. Only cells with series resistance between 10 and 20 MΩ were used for analysis. The cell capacitance of HL-60 granulocytes was between 4 and 5 pF.

Measurement of cytosolic free [Ca²⁺]_i in patched cells

Cytosolic free Ca²⁺ concentration, [Ca²⁺]_i, in patched cells was measured using the fluorescent [Ca²⁺] indicator indo-1 as previously described (Demaurex et al., 1992). Note that indo-1 was introduced into cells i) as indo-1 AM before the experiment and ii) as indo-1 free acid through the patch pipette. This procedure allows measurement of [Ca²⁺]_i at early time points after break-in. On the stage of an inverted microscope equipped for indo-1 measurements (Nikon Diaphot; all optics are from Nikon Corp., Tokyo, Japan), the excitation light, provided by a mercury lamp, was first attenuated 256 times (two neutral density filters of 16), then passed through a 355 ± 5 nm interference filter, and was reflected to the stage (dichroic mirror 380 nm). The emitted fluorescence was split in two by a second dichroic mirror (455 nm), and the light intensity was measured at 405 ± 5 nm and 480 ± 5 nm (selected by interference filters) on two P1 photometers (Hamamatsu, Japan). Recording of the photometric data was performed at a rate of 50 Hz using a 12-bit analog/digital (A/D) board (Acqui, SICMU, Centre Médical Universitaire, Geneva) interfaced to a PC/AT computer. *R*, the ratio of the emitted fluorescences at 405 nm and 480 nm, was calculated, and [Ca²⁺]_i was derived using the equation

$$[\text{Ca}^{2+}]_i = K_d * \beta * (R - R_{\min}) / (R_{\max} - R)$$

R is the ratio of the indo-1 emitted fluorescences at two wavelengths (*F*₄₀₅/*F*₄₈₀). *R*_{min} = 0.025 ± 0.005 (*n* = 6) was measured as the *R* value after break-in with a pipette solution containing 10 mM EGTA (Almers and Neher, 1985). *R*_{max} = 0.35 ± 0.01 (*n* = 8) was determined as the *R* value of intact cells incubated with 2 μM ionomycin in the presence of 10 mM CaCl₂. *K*_d * β = 1280 ± 40 (*n* = 6) was determined after break-in with a pipette solution heavily buffered at 300 nM Ca²⁺ (9.2 mM EGTA and 5.4 mM CaCl₂). All experiments were performed at room temperature.

Preparation of cell homogenates, crude membranes, subcellular fractions, and permeabilized cells

HL-60 cells were permeabilized or homogenized and fractionated as previously described; [³²P]-Ins(1, 4, 5)P₃ binding, ⁴⁵Ca²⁺ measurements, and fura-2 measurements were performed as previously detailed (Van Delden et al., 1992a, 1993). Two different approaches were used to measure Ca²⁺ release in permeabilized cells, homogenates, or subcellular fractions: the fura-2 technique and the ⁴⁵Ca²⁺ technique. For detailed description of the techniques see previous publications (Van Delden et al., 1992b; Favre et al., 1994). However, the following points, important for the interpretation of this study, should be mentioned. For both techniques, the identical incubation medium, mimicking intracellular ionic conditions (KCl 120 mM, MgCl₂ 1 mM, HEPES 25 mM, pH 7.0) was used, including an ATP-regenerating system (MgATP 1 mM, creatine phosphate 2.5 mM, creatine kinase 4 U ml⁻¹) and mitochondrial inhibitors (antimycin 0.2 μM

and oligomycin 1 mg ml⁻¹). However, for the fura-2 experiments, 2 μM fura-2 was added to the incubation medium, and Ca²⁺ release was measured as a change in the medium free Ca²⁺ concentration. In contrast, for the ⁴⁵Ca²⁺ experiments, 1 mM HEDTA was added to the incubation medium; thus the free Ca²⁺ concentration in the medium did not change, and Ca²⁺ release was measured as a change in the Ca²⁺ content of Ca²⁺ stores. With both techniques, the time resolution was relatively low (>10 s), and the results therefore are steady-state values and not initial flux rates. The response to a given Ins(1, 4, 5)P₃ concentration was defined as the peak value of [Ca²⁺]_i, changes after Ins(1, 4, 5)P₃ addition (fura-2 experiments) or as the steady-state value of decreased Ca²⁺ store content observed 1 min after Ins(1, 4, 5)P₃ addition (⁴⁵Ca²⁺ experiments).

Analysis and statistics

Recorded data were transferred and analyzed in the package Origin (MicroCal Software Inc., Northampton, MA), implemented with LabTalk routines when necessary. After selection of the data to be fitted, a smoothing on 21 points by adjacent averaging was performed and the initial estimates for the free parameters were determined by eye. Three free variables were fitted by the Hill equation (Eq. 1): *y*_{max}, *K*_d and *n* (details in Appendix). No weighting factor was used. Analysis was performed on a PC/AT 486 computer and required approximately 200 to 400 iterations to achieve a stable condition. For statistical comparisons between different conditions a Wilcoxon sign rank test with a level of significance α = 0.05 was used. For multiparameter fitting analysis, data were transferred into the software Matlab (The MathWorks Inc., Natick, MA). Data were selected between the rupture of the patch membrane (= establishing the whole-cell configuration) and the break point determined on the first derivative. No weighting factor was used in the absence of any heteroscedasticity (= change in variance across time). The [Ca²⁺]_i at time 0 was determined by averaging on 21 points. Initial estimates for the variables *y*_{max(HE2)}, *y*_{max(HE3)}, *EC*_{50(HE2)}, and *EC*_{50(HE3)} were determined by eye (details in Appendix). Minimization procedures for the fitting were based on the simplex method (nonlinear least-squares regression method). Computation required approximately 600 to 1200 iterations to achieve a stable condition with a level of confidence of 1%. The quality of the fit was assessed by the *F*-test, which compares the ratio between the explained variance (variance of the data minus residuals) and the residuals (data minus fit) (Patel et al., 1976).

Reagents

Digitonin, thapsigargin, and dimethylsulfoxide (DMSO) were purchased from Sigma (St. Louis, MO), fetal calf serum from Gibco (Paisley, Scotland), Percoll from Pharmacia (Uppsala, Sweden), ⁴⁵Ca²⁺ and [³²P]-Ins(1, 4, 5)P₃ from Du Pont de Nemours/NEN (Dreieich, Germany), fura-2 pentasodium salt (free acid form) from Calbiochem (La Jolla, CA), and indo-1 acetoxyethyl ester (indo-1 AM) from Molecular Probes (Eugene, OR). For patch-clamp experiments: inositol 1,4,5-trisphosphate (Ins(1, 4, 5)P₃) and its poorly metabolizable analog Ins(2, 4, 5)P₃ (>99% pure) were isolated and purified according to the method of Henne et al. (1988). Ins(1, 4, 5)P₃ used in broken cell experiments was from Amersham International (Buckinghamshire, England). All other chemicals were of analytical grade and were obtained from Amersham, Calbiochem, Sigma, Merck (Darmstadt, Germany), and Fluka (Buchs, Switzerland). The patch-clamp medium referred to as "Ca²⁺ medium" contained (in mM): NaCl 138; KCl 6; CaCl₂ 1.1; MgCl₂ 1; EGTA 0.1; glucose 20; HEPES 20; pH 7.4. The Ca²⁺-free medium had the same ionic composition; however, it contained 1 mM EGTA, and CaCl₂ was omitted.

RESULTS AND ANALYSIS

It was the purpose of this study to investigate whether a [Ca²⁺]_i increase in response to Ins(1, 4, 5)P₃ is a coopera-

tive process. As in its classical, linearized form, the Hill equation depends strongly on the assumed maximum, we obtained Hill coefficients by computer fitting of the concentration-response curves to the Hill equation in its non-linear form (Barlow and Blake, 1989; see also Discussion):

$$y = \frac{y_{\max}}{1 + (EC_{50}/[i]_i)^n} \quad (1)$$

This approach has been widely used not only for the analysis of binding constants, but also for the analysis of concentration-response curves (Varnai et al., 1993; Nunn and Taylor, 1990; Facklam et al., 1992).

Ins(1, 4, 5)P₃ binding to membranes from HL-60 granulocytes and Ins(1, 4, 5)P₃-induced Ca²⁺ release from HL-60 homogenates

We first investigated Ins(1, 4, 5)P₃ binding to a crude membrane fraction from HL-60 granulocytes using a radioligand binding assay. Similar to previous observations in other cellular systems (Spät et al., 1986; Mauger et al., 1994; Worley et al., 1989), the binding is not cooperative (Table 1). This does not necessarily contradict the concept of a cooperativity of Ins(1, 4, 5)P₃-induced Ca²⁺ release, as the cooperativity might be on the level of pore opening, rather than on the level of the ligand subunit interaction (Meyer et al., 1988, 1990). For the rest of this study we have therefore investigated Ins(1, 4, 5)P₃-induced Ca²⁺ release and its possible cooperativity. Most commonly, Ins(1, 4, 5)P₃-induced Ca²⁺ release is studied in cell homogenates using ⁴⁵Ca²⁺ or fluorescent probes. We have used both techniques to obtain concentration-response curves of Ins(1, 4, 5)P₃-induced Ca²⁺ release and found with both techniques Hill coefficients close to 1, suggesting a noncooperative process (Table 1). The absence of cooperativity in both assay systems provides important information. The ⁴⁵Ca²⁺ measurements were performed in heavily Ca²⁺-buffered extracellular solutions, whereas the fura-2 measurements were performed without added Ca²⁺ buffers. Thus, the Ca²⁺ concentration in the medium (which is the experimental equivalent of the cytosolic free Ca²⁺ concentration, [Ca²⁺]_i) was clamped during Ins(1, 4, 5)P₃-induced Ca²⁺ release in the ⁴⁵Ca²⁺ experiments, but increased to

values around 550 nM in the fura-2 experiments. The absence of cooperativity in the ⁴⁵Ca²⁺ experiments suggested that a putative cooperativity was not simply overlooked because of a negative feedback by [Ca²⁺]_i elevations. The absence of cooperativity in the fura-2 experiments suggested that we had not simply overlooked a putative cooperativity due to a positive feedback by [Ca²⁺]_i (which would remain undetected in the ⁴⁵Ca²⁺ experiments). When digitonin-permeabilized cells or partially purified intracellular Ca²⁺ stores were tested, similar noncooperative concentration-response curves were observed (Table 1).

Thus, neither the binding studies of HL-60 membranes nor the ⁴⁵Ca²⁺ or fura-2 measurements in homogenates or permeabilized cells provided arguments in favor of a cooperativity of the Ins(1, 4, 5)P₃ response. However, for the following reasons, these results do not exclude a cooperativity of Ins(1, 4, 5)P₃-induced Ca²⁺ release:

i) The cooperativity of Ins(1, 4, 5)P₃-binding or Ins(1, 4, 5)P₃-induced channel opening might go unrecognized because of the existence of different populations of Ca²⁺ stores that are heterogeneous with respect to their affinity for Ins(1, 4, 5)P₃ (Taylor, 1992) or the heterogeneity of different cells with respect to their sensitivity to Ins(1, 4, 5)P₃ (Bootman et al., 1992).

ii) The ⁴⁵Ca²⁺ and fura-2 measurements in both permeabilized cells and cell homogenates have a relatively poor time resolution. Thus, the studies performed so far have taken into account a steady-state Ca²⁺ release, rather than an initial rate of Ca²⁺ efflux in response to Ins(1, 4, 5)P₃ and will therefore measure in addition to opening of the channel a variety of other effects (e.g., diminished driving force due to store depletion, negative feedback mechanisms, activation of the Ca²⁺-ATPase, etc.)

Kinetics of [Ca²⁺]_i elevations in response to microperfusion of Ins(1, 4, 5)P₃

Taking into account the considerations outlined above, it becomes clear that the ideal experimental conditions for the assessment of the cooperativity of Ins(1, 4, 5)P₃-induced Ca²⁺ release would be the determination of the initial kinetics of Ins(1, 4, 5)P₃-induced Ca²⁺ release with high time resolution in a single cell. We therefore considered the

TABLE 1 Synopsis of Hill coefficients of Ins(1, 4, 5)P₃ concentration-response curves in HL-60 granulocytes under various experimental conditions

Material	Type of assay	InsP ₃ isomer	<i>n</i>	<i>N</i>
Crude membranes	Radioligand binding, steady state	Ins(1,4,5)P ₃	0.97 ± 0.11	5
Homogenates	⁴⁵ Ca ²⁺ release, steady state	Ins(1,4,5)P ₃	1.17 ± 0.13	3
Homogenates	Fura-2, steady state	Ins(1,4,5)P ₃	1.22 ± 0.16	3
Permeabilized cells	⁴⁵ Ca ²⁺ release, steady state	Ins(1,4,5)P ₃	1.06 ± 0.74	3
8-fold purified Ca ²⁺ stores	Fura-2, steady state	Ins(1,4,5)P ₃	1.17 ± 0.14	5
Patch-clamped single cell	Indo-1, onset kinetics, [Ca ²⁺] _o = 2mM	Ins(1,4,5)P ₃	8.1 ± 1.8	13
Patch-clamped single cell	Indo-1, onset kinetics, [Ca ²⁺] _o < 1 μM	Ins(1,4,5)P ₃	8.9 ± 1.9	5
Patch-clamped single cell	Indo-1, onset kinetics, [Ca ²⁺] _o = 2mM	Ins(2,4,5)P ₃	8.9 ± 1.1	8

For detailed description, see Materials and Methods.

possibility of using the whole-cell patch-clamp technique, combined with microfluorimetry to study the rapid kinetics of Ins(1, 4, 5)P₃-induced [Ca²⁺]_i elevations. To assess the feasibility of this approach, we first modeled Ins(1, 4, 5)P₃-induced Ca²⁺ release under these experimental conditions. The microperfusion of small compounds into whole-cell patch-clamp cells can be described as a single exponential decay (Pusch and Neher, 1988).

$$[\text{InsP}_3]_i = [\text{InsP}_3]_p * (1 - e^{-t/\tau}) \quad (2)$$

[InsP₃]_i is the (variable) cytosolic InsP₃ concentration, [InsP₃]_p the (constant) InsP₃ concentration in the patch pipette, *t* the time (in seconds) after break-in, and τ is the time constant (in seconds) for the InsP₃ microperfusion into the cytosol. As *t* is the variable of the equation and [InsP₃]_p an experimentally set constant, the only unknown of the equation is τ . The time constant τ depends on three parameters: the pipette tip limitation, the cytosolic volume of the microperfused cell, and the velocity of diffusion of the compound. Two parameters determined during a patch-clamp experiment, access resistance (*R*_A, between 10 and 20 M Ω in our experiments) and the whole-cell capacitance (*C*, between 4 and 5 pF for HL-60 granulocytes, from which volume may be calculated assuming a spherical cell), provide estimates for the pipette tip limitation and the cytosolic volume of the microperfused cells, respectively. The velocity of diffusion of Ins(1, 4, 5)P₃ has been experimentally

determined in the cytosol of *Xenopus laevis* oocytes ($D = 283 \mu\text{m}^2 \cdot \text{s}^{-1}$; Allbritton et al., 1992).

Using the following theoretically predicted (Oliva et al., 1988; Mathias et al., 1990) and experimentally confirmed (Pusch and Neher, 1988) equation

$$\tau = (C/5.9)^{1.5} * (784 \pm 66) * R_A/D \quad (3)$$

we were able to estimate τ values between 10 and 40 s for the microperfusion of Ins(1, 4, 5)P₃ into whole-cell patch-clamped HL-60 granulocytes (assuming a *D* of $283 \mu\text{m}^2 \cdot \text{s}^{-1}$, a *C* of 4.5 pF, and a *R*_A between 10 and 20 M Ω). Fig. 1 A shows the predicted time course of the increase of Ins(1, 4, 5)P₃ in the cytosol of an HL-60 granulocyte during a whole-cell patch-clamp experiment for this range of time constants.

By combining Eqs. 1 and 3, we can now model the Ca²⁺ release in response to Ins(1, 4, 5)P₃ microperfusion into an HL-60 granulocyte. As shown in Fig. 1, B–D, the kinetics of the expected Ca²⁺ release (expressed as a percentage of the maximum) depends on i) the InsP₃ concentration in the pipette, ii) the time constant of Ins(1, 4, 5)P₃ microperfusion, iii) the EC₅₀ of Ins(1, 4, 5)P₃-induced Ca²⁺ release, and iv) the cooperativity of Ins(1, 4, 5)P₃-induced Ca²⁺ release. However, although all four parameters were able to influence the kinetics of Ins(1, 4, 5)P₃-induced Ca²⁺ release, only a change in cooperativity was able to influence the shape of the curve. In this setting, the curve for a

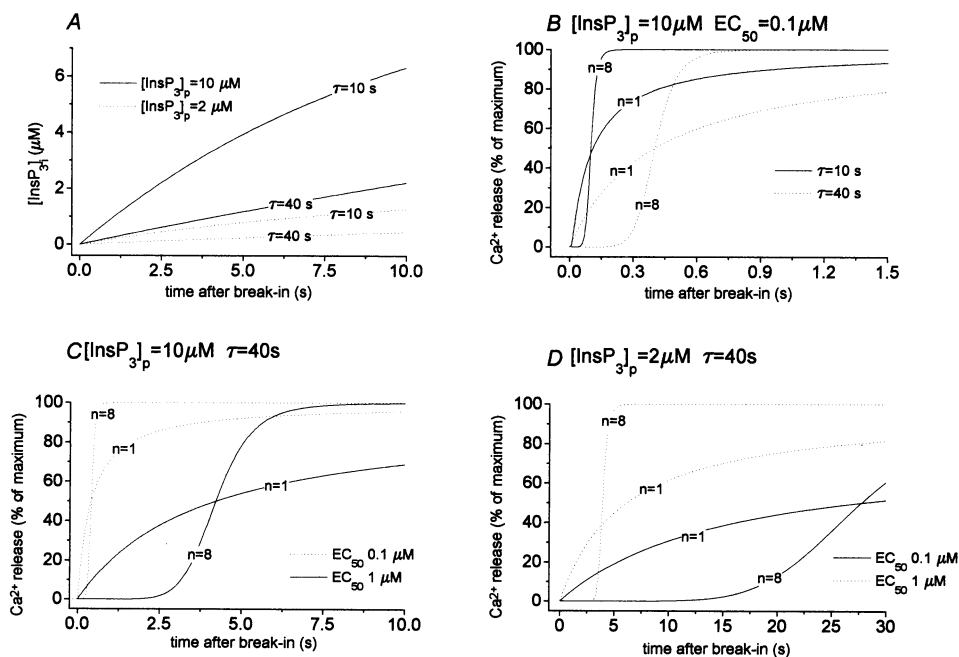


FIGURE 1 Modeling of Ins(1, 4, 5)₃-induced Ca²⁺ release in response to Ins(1, 4, 5)P₃ microperfusion in a whole-cell patch clamp experiment. (A) [InsP₃]_i (= cytosolic InsP₃ concentration) at a given time after break-in was calculated as a function of τ (τ = time constant for InsP₃ diffusion into the cytosol) and [InsP₃]_p (= InsP₃ concentration in the pipette) (see Eq. 2). (B–D) InsP₃-induced Ca²⁺ release (percentage of maximum) at a given InsP₃ concentration was modeled using a Hill equation (Eq. 1) with *n* (= Hill coefficient) and EC₅₀ (= InsP₃ concentration eliciting half-maximal Ca²⁺ release) as variables. The break-in (= rupture of the patch membrane to obtain the whole-cell patch-clamp configuration) was defined as 0 s. (B) Effect of two different Hill coefficients and time constants on the kinetics of InsP₃-induced Ca²⁺ release for [Ins(1, 4, 5)P₃]_p = 10 μM, and EC₅₀ = 0.1 μM. (C) Effect of two different Hill coefficients and two different EC₅₀ on the kinetics of InsP₃-induced Ca²⁺ release for [Ins(1, 4, 5)P₃]_p = 10 μM, and τ = 40 s. (D) As in C, but [Ins(1, 4, 5)P₃]_p = 2 μM. Note the different x axis scales.

noncooperative Ca^{2+} release is always hyperbolic, whereas a cooperative Ca^{2+} release will always lead to a sigmoidal curve. Thus, our modeling suggests that the whole-cell patch clamp is a useful approach for the analysis of the cooperativity of the $\text{Ins}(1, 4, 5)\text{P}_3$ response.

We therefore performed whole-cell patch-clamp experiments to microperfuse single HL-60 granulocytes with $\text{Ins}(1, 4, 5)\text{P}_3$ and measured $[\text{Ca}^{2+}]_i$ responses by double-emission microfluorimetry using indo-1. Preloading of the cells with indo-1 allowed measurement of the early changes in $[\text{Ca}^{2+}]_i$ without any delay for the microperfusion of the dye. Fig. 2 shows the initial kinetics of the $[\text{Ca}^{2+}]_i$ increase (Fig. 2, A and B) in cells microperfused with $10 \mu\text{M}$ $\text{Ins}(1, 4, 5)\text{P}_3$ in either Ca^{2+} medium (left column) or Ca^{2+} -free conditions (right column). As the biologically relevant parameter is the rate of $[\text{Ca}^{2+}]_i$ increase, we calculated the first derivative of the $\text{Ins}(1, 4, 5)\text{P}_3$ -induced $[\text{Ca}^{2+}]_i$ increase, $d[\text{Ca}^{2+}]_i/dt$.

Then, as a given time point after break-in corresponds to a given $\text{Ins}(1, 4, 5)\text{P}_3$ concentration (see Fig. 1 A), we converted the x axis into $[\text{Ins}(1, 4, 5)\text{P}_3]$ (in μM) using Eq. 2 (Fig. 2, C–D). For this example we assumed a τ of 40 s for the microperfusion of $\text{Ins}(1, 4, 5)\text{P}_3$; in the following mathematical analysis, the influence of the assumed time constant on the obtained Hill value will be carefully evaluated (see below).

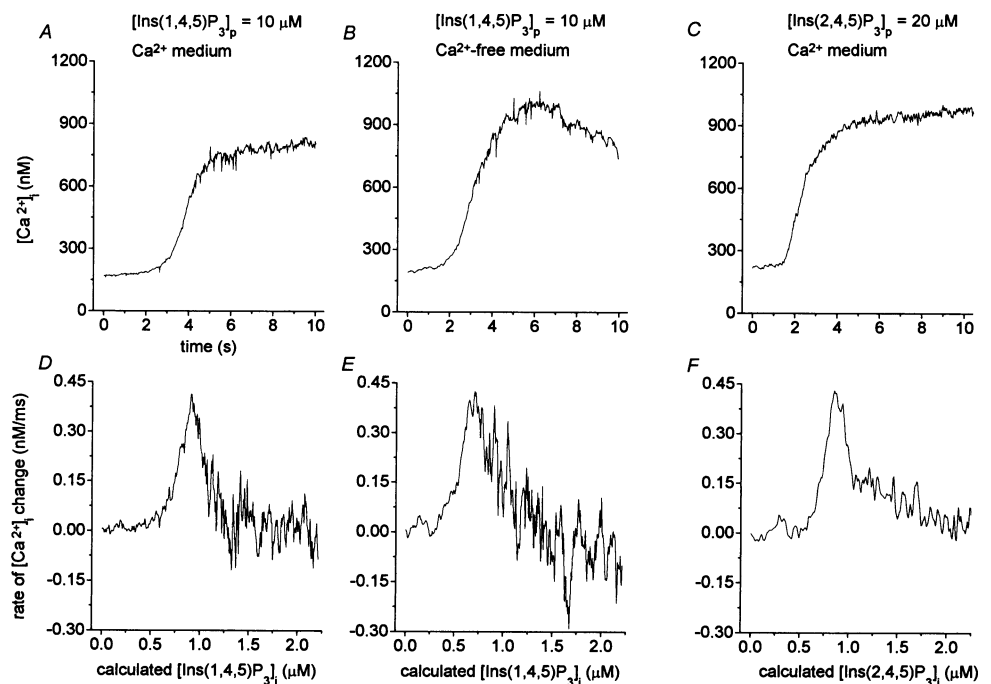
Fig. 2 shows typical examples of the rate of $[\text{Ca}^{2+}]_i$ increase after $\text{Ins}(1, 4, 5)\text{P}_3$ microperfusion in Ca^{2+} -containing or Ca^{2+} -free medium (Fig. 2, C and D, respectively). Without exception, the visual inspection of all traces revealed three phases (see also Fig. 3 A): phase 1 was an apparent lag time, and phase 2 and phase 3 were characterized by a rapid acceleration and decline in the rate of

$[\text{Ca}^{2+}]_i$ elevations, respectively. Whereas the transition between phase 1 and phase 2 was smooth, there was an abrupt transition between phases 2 and 3, with the visual impression of a break point. This break point was a prominent feature of all traces that were analyzed and might possibly reflect the onset of negative feedback mechanisms. For our analysis, aiming to study the early kinetics of the $\text{Ins}(1, 4, 5)\text{P}_3$ response, the break point has been a useful tool. Phases 1 and 2 (i.e., the time between the achievement of the whole-cell configuration and the break point) were defined as the early $\text{Ins}(1, 4, 5)\text{P}_3$ response and exclusively used for all subsequent analysis. Visual inspection of the traces after conversion of time into $\text{Ins}(1, 4, 5)\text{P}_3$ concentration (Fig. 2, C and D) revealed another important aspect. The increase in the rate of $[\text{Ca}^{2+}]_i$ elevations in phase 2 of the traces was far higher than the increase in the $\text{Ins}(1, 4, 5)\text{P}_3$ concentration: for a doubling of the $\text{Ins}(1, 4, 5)\text{P}_3$ concentration (e.g., from 0.4 to $0.8 \mu\text{M}$), a more than tenfold increase in the rate of $[\text{Ca}^{2+}]_i$ elevations was observed. To quantify these observations, we used two different analytical approaches: i) we fitted Eq. 1 to phases 1 and 2 of the $\text{Ins}(1, 4, 5)\text{P}_3$ -induced $[\text{Ca}^{2+}]_i$ elevations (= curve fitting analysis), and ii) we analyzed the steepness of the concentration-response curve in phase 2 of the $\text{Ins}(1, 4, 5)\text{P}_3$ -induced $[\text{Ca}^{2+}]_i$ elevations (= steepness analysis).

Curve-fitting analysis of the onset of $\text{Ins}(1, 4, 5)\text{P}_3$ -induced $[\text{Ca}^{2+}]_i$ elevations

For this analysis, phase 1 and phase 2 of the $[\text{Ca}^{2+}]_i$ elevations curves were fitted by Eq. 1 (Fig. 3 A). Mean n

FIGURE 2 $[\text{Ca}^{2+}]_i$ elevations in response to microperfusion of $10 \mu\text{M}$ $\text{Ins}(1, 4, 5)\text{P}_3$ or $20 \mu\text{M}$ of its poorly hydrolyzable analog $\text{Ins}(2, 4, 5)\text{P}_3$. Indo-1 loaded granulocytes were voltage-clamped at -60 mV in the whole-cell patch clamp configuration. Time 0 denotes time after break-in. (A–C) Original recordings of $[\text{Ca}^{2+}]_i$ elevations as a function of time in response to microperfusion of InsP_3 . (D–F) The first derivative was calculated and plotted as a function of $[\text{InsP}_3]_i$. Time was converted to $[\text{InsP}_3]_i$, assuming a time constant of 40 s (Eq. 2). Experiments were either performed in a Ca^{2+} -containing medium (A and C) or in a Ca^{2+} -free medium (B). Traces are representative of 13, 5, and 8 experiments for A, B, and C, respectively.



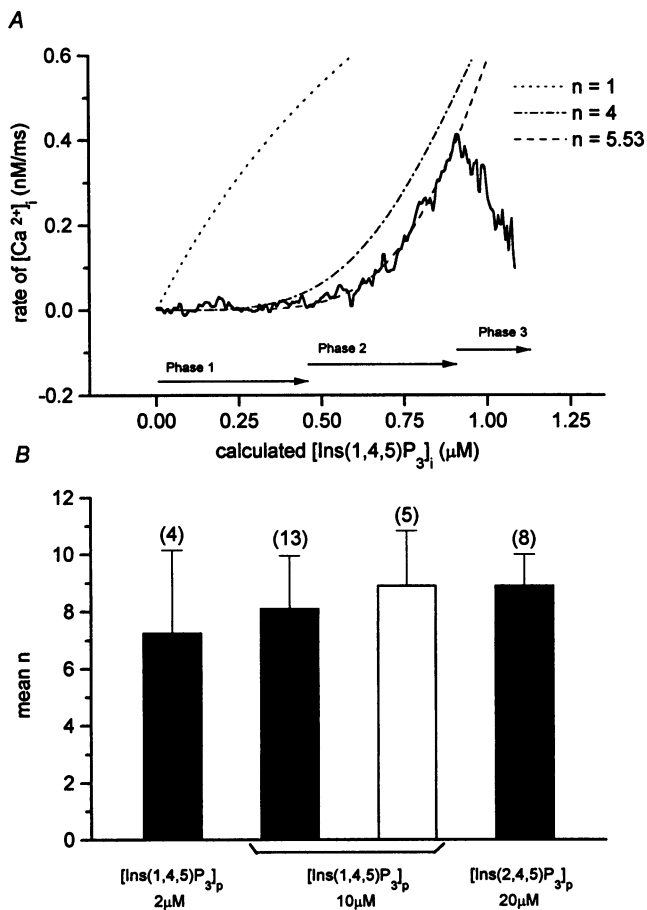


FIGURE 3 Curve fitting analysis of $[Ca^{2+}]_i$ elevations in response to microperfusion of Ins(1, 4, 5)P₃. Experiments were performed as described in Fig. 2. Phase 1 and phase 2 were analyzed by a best-fit procedure with a Hill equation in its nonlinear form. For this trace, a Hill coefficient of 5.53 was obtained. For comparison, calculated curves with Hill coefficients of 1 and 4 are shown in the same panel. (B) average Hill coefficients under various experimental conditions. Ins(1, 4, 5)P₃ concentrations and isomers are indicated on the x axis. Black bars indicate experiments performed in a Ca²⁺-containing medium, and the white bar indicates experiments in a Ca²⁺-free medium. Data are mean \pm SE of 4, 13, 5, and 8 experiments (columns 1, 2, 3, 4, respectively). The assumed time constant was 40 s.

values of the obtained results under different experimental conditions are shown in Fig. 3 B and in Table 1. We first analyzed experiments where 10 μ M Ins(1, 4, 5)P₃ was microperfused (as shown in Fig. 2). The Hill coefficient of the Ins(1, 4, 5)P₃-induced $[Ca^{2+}]_i$ elevations was 8.1 ± 1.8 ($n = 13$) in a Ca²⁺-containing medium. Thus, the onset of Ins(1, 4, 5)P₃-induced $[Ca^{2+}]_i$ elevations observed in a single granulocyte was highly cooperative. If our modeling was correct, the obtained n values should be independent of the Ins(1, 4, 5)P₃ concentration in the pipette ($[Ins(1, 4, 5)P_3]_p$). Thus, when a lower $[Ins(1, 4, 5)P_3]_p$ is used, a slower ramp of $[Ins(1, 4, 5)P_3]_i$ will be generated by the microperfusion; however, the basic characteristics of the concentration-response curve should be preserved. Indeed, the n values calculated from experiments with an $[Ins(1, 4, 5)P_3]_p$ of 2 μ M were virtually identical to the n

values calculated from experiments with an $[Ins(1, 4, 5)P_3]_p$ of 10 μ M (7.3 ± 2.9 , $n = 4$; Fig. 3 B). When 10 μ M Ins(1, 4, 5)P₃ was microperfused in a Ca²⁺-free medium, a similar Hill coefficient (8.9 ± 1.9 , $n = 5$; Fig. 3 B) was observed, suggesting that the observed cooperativity was only due to Ca²⁺ release and did not depend on the activation of Ca²⁺ influx. Metabolism of Ins(1, 4, 5)P₃ might generate other inositol phosphates that activate Ca²⁺ release, and this metabolism might underlay the observed cooperativity. We therefore performed experiments with the poorly metabolizable InsP₃ isomer Ins(2, 4, 5)P₃ (Fig. 2, C and F; Fig. 3 B). Similar Hill coefficients (8.9 ± 1.1 ; $n = 8$) were obtained. Thus, Ins(1, 4, 5)P₃ metabolism does not appear to be involved in the mechanism of cooperativity of the Ins(1, 4, 5)P₃ response.

Steepness analysis of Ins(1, 4, 5)P₃-induced $[Ca^{2+}]_i$ elevations

The results of the curve-fitting analysis clearly suggest a high cooperativity of Ins(1, 4, 5)P₃-induced $[Ca^{2+}]_i$ elevations. The curve-fitting analysis uses both the lag time and the shape (i.e., steepness) of the Ins(1, 4, 5)P₃ response. In a second approach, referred to as steepness analysis, we have analyzed the data independently of the lag time. The Hill coefficient affects the steepness of the concentration-response curve, and one may define (outlined mathematically in the Appendix) this steepness as the fold increase of the response upon a doubling in agonist concentration. Thus, in the case of the Ins(1, 4, 5)P₃ response, the increase in the rate of $[Ca^{2+}]_i$ elevations in response to a doubling of the Ins(1, 4, 5)P₃ concentration is a measure of the steepness, and therefore of the Hill coefficient, of the concentration-response curve (for a graphical example see Fig. 4 A).

Mathematically, the steepness of the concentration-response curve may be expressed as detailed in the Appendix. y_x is defined as the response at the cytosolic $[Ins(1, 4, 5)P_3] = x$, and y_{2x} as the response at double the cytosolic $[Ins(1, 4, 5)P_3] = 2x$ (Fig. 4 A). For concentrations clearly below the EC₅₀, the base 2 logarithm of y_{2x}/y_x is then an approximation of the n (Fig. 4 B; note that analysis close to or above the EC₅₀ will lead to an underestimation but not to an overestimation of n). The ratio y_{2x}/y_x from our experimental data was obtained by computed analysis of phase 2 of the $[Ca^{2+}]_i$ elevations curve. The y_{2x}/y_x values of each recording (7–12 values per trace) were averaged and are shown in Fig. 4 C. Independently of the presence or absence of extracellular Ca²⁺ and of the use of hydrolyzable or nonhydrolyzable InsP₃ analogs, the y_{2x}/y_x ratios were above 20, suggesting a high cooperativity of the curve. The results did not change when the median of the ratios y_{2x}/y_x was used instead of the mean (36.0 ± 12.0 versus 36.7 ± 13.1), demonstrating the robustness of the data.

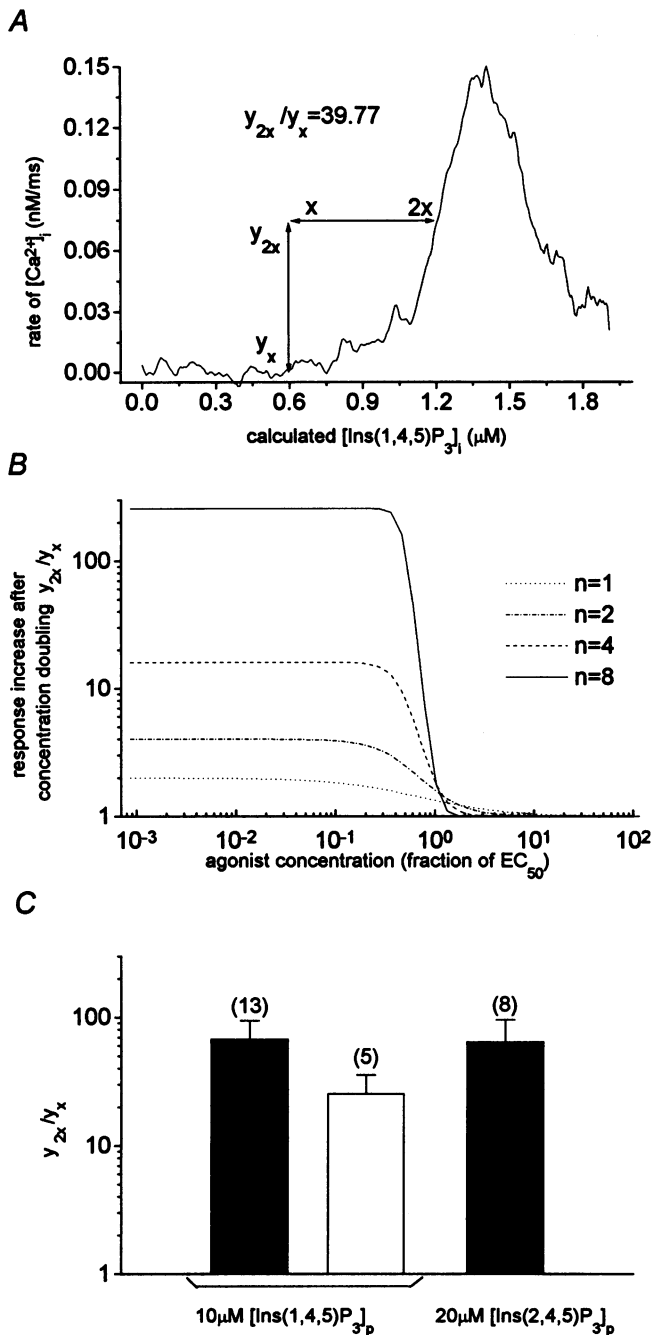


FIGURE 4 Steepness analysis of $[Ca^{2+}]_i$ elevations in response to microperfusion of $Ins(1, 4, 5)P_3$. (A) An HL-60 granulocyte was microperfused with $10 \mu M$ $Ins(1, 4, 5)P_3$ in a Ca^{2+} -containing medium. The rate of Ca^{2+} release as a function of $[Ins(1, 4, 5)P_3]_i$ was obtained as shown in Fig. 2. y_x is the rate of $[Ca^{2+}]_i$ increase at a given $[Ins(1, 4, 5)P_3]_i (= x)$, and y_{2x} is the rate at the double $[Ins(1, 4, 5)P_3]_i (= 2x)$. The ratio y_{2x}/y_x is a measure of the steepness of the curve, i.e., an indicator of cooperativity. (B) Calculated y_{2x}/y_x values as a function of agonist concentration (expressed as a fraction of the EC_{50}) for various Hill values. Note that for agonist concentrations below the EC_{50} , y_{2x}/y_x evolves against 2^n . (C) Average y_{2x}/y_x values under various experimental conditions. Computed analysis allowed us to obtain 7–12 y_{2x}/y_x values per cell, which were averaged. $Ins(1, 4, 5)P_3$ concentrations and isomers are indicated on the x axis. Black bars indicate experiments performed in a Ca^{2+} -containing medium, and the white bar indicates experiments in a Ca^{2+} -free medium. Data are mean \pm SE of 13, 5, and 8 experiments (columns 1, 2, 3, respectively). The assumed time constant was 40 s.

Influence of the assumed time constant on the obtained Hill coefficient

As outlined above, the only value used in our analysis that was not strictly experimentally derived is τ , the time constant of $Ins(1, 4, 5)P_3$ microperfusion. Previous theoretical and experimental work allowed us to estimate a reasonable range of time constants (between 10 and 40 s); however, it did not allow us to obtain one precise value. In previous patch-clamp experiments in human neutrophil granulocytes (Nüsse and Lindau, 1993), the experimentally determined time constants of fura-2 microperfusion ranged between 25 and 60 s (for access resistances between 10 and 20 $M\Omega$).

As no technique is currently available to measure directly the microperfusion of $Ins(1, 4, 5)P_3$ into a patch-clamp cell, it was important to analyze the influence of the assumed time constant on the obtained Hill coefficients. For this purpose we have converted the x axis of our microperfusion data from time (s) into $[Ins(1, 4, 5)P_3]_i$ (μM) (as shown in Fig. 2, C and D), assuming various time constants between 10 and 60 s, and reanalyzed the data. The values obtained by curve-fitting analysis showed only a minor dependence on the assumed time constant (n ranging from 9.4 ± 2.3 to 8.0 ± 1.8 , $n = 13$) and were virtually independent of τ in the steepness analysis (range of y_{2x}/y_x : 23.8 ± 0.4 to 22.4 ± 0.3 , $n = 13$) (Fig. 5). Thus, independent of the assumed time constant, our results show a high cooperativity of $Ins(1, 4, 5)P_3$ -induced $[Ca^{2+}]_i$ elevations.

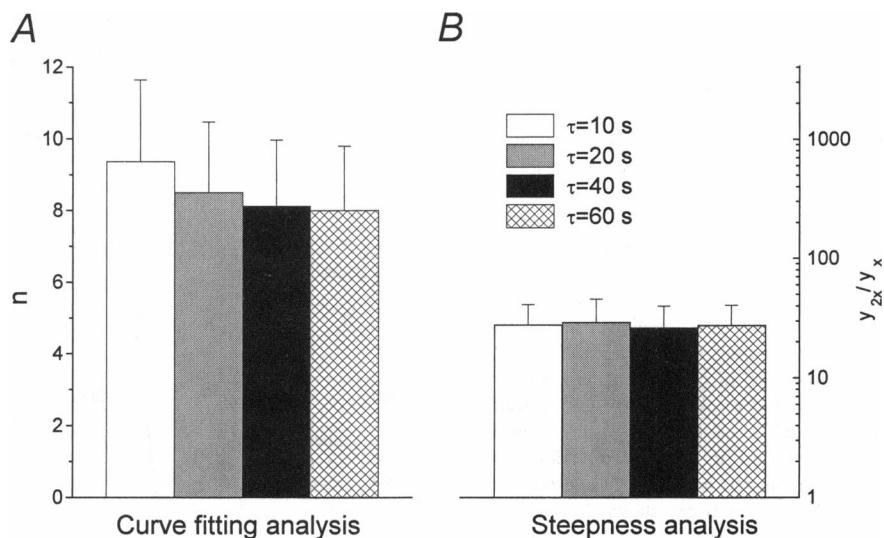
Lag time analysis

Long lag times are a typical feature of cooperative systems, and we had indeed measured relatively long lag times in response to $Ins(1, 4, 5)P_3$ microperfusion in a previous study (Demaurex et al., 1992). We have therefore developed mathematical models to define the factors that determine the lag time in our system (not shown). The modeling demonstrated that the lag time depends not only on the cooperativity, but also strongly on the EC_{50} of the $Ins(1, 4, 5)P_3$ -response, the time constant of microperfusion, and the threshold of detection of $[Ca^{2+}]_i$ elevations. Thus, although the relatively long lag times observed after $Ins(1, 4, 5)P_3$ microperfusion in our system are compatible with the concept of cooperativity, they could not be used for a direct determination of the cooperativity.

Multiparameter fitting analysis, weighting the potential contribution of cooperativity on the level of channel opening and on the level of Ca^{2+} feedback

Cooperativity is a phenomenon that describes the steepness of a binding curve (free ligand versus bound ligand) or the steepness of a concentration-response curve (free ligand versus biological response). In binding studies, a positive cooperativity is generally thought to represent the presence of multiple binding sites, where occupation of one site

FIGURE 5 Effect of τ , the assumed time constant for InsP₃ diffusion, on the observed cooperativity. Microperfusion of an HL-60 granulocyte with 10 μ M Ins(1, 4, 5)P₃ in a Ca²⁺-containing medium. (A) [Ca²⁺]_i elevations were fitted with a Hill equation as described in Fig. 3, but assuming various time constants for InsP₃ diffusion into the cytosol. Hill coefficients \pm SE were 9.4 ± 2.3 , 8.5 ± 2.0 , 8.1 ± 1.8 , and 8.0 ± 1.8 ($n = 13$), for a time constant of 10, 20, 40, and 60 s, respectively. (B) The steepness of [Ca²⁺]_i elevations was analyzed as described in Fig. 4, using different τ values. Calculated response increases after concentration doubling (y_{2x}/y_x) were 22.7 ± 0.4 , 23.8 ± 0.4 , 22.4 ± 0.3 , and 23.2 ± 0.3 ($n = 13$), for a τ of 10, 20, 40, and 60 s, respectively.



facilitates binding to another. In the case of functional concentration-response studies, the mechanisms that may account for steep (i.e., cooperative) curves can be more complex. Cooperativity in this context may not necessarily be due to a cooperativity of binding, but basically to any positive feedback response of the function under investigation. In the case of Ins(1, 4, 5)P₃-induced [Ca²⁺]_i elevations, the most likely candidates to cause cooperativity are cooperativity on the level of channel opening (i.e., channel opening occurs only when all four subunits of the Ins(1, 4, 5)P₃ receptor are occupied; see Meyer et al., 1990) or cooperativity due to positive Ca²⁺ feedback (Bezprozvanny et al., 1991). The two types of cooperativity will be referred to as $n(\text{channel})$ and $n(\text{Ca}^{2+})$, respectively, throughout the text. Given the very high overall cooperativity observed in our experiments ($n \approx 8$; see Fig. 3), we had to take into consideration the possibility that both contributed to the observed steepness of the curve. We therefore developed a computed analysis that integrates the Ins(1, 4, 5)P₃ concentration response for Ca²⁺ release, as well as a Ca²⁺ concentration response for the positive feedback on Ins(1, 4, 5)P₃-induced Ca²⁺ release. The analysis consists of three interconnected Hill equations: HE1: Ins(1, 4, 5)P₃-dependence of [Ca²⁺]_i elevations; HE2: Ca²⁺ dependence of the maximum of the Ins(1, 4, 5)P₃ concentration response; HE3: Ca²⁺ dependence of the EC₅₀ of the Ins(1, 4, 5)P₃ response (a Ca²⁺ dependence of both maximum and EC₅₀ of the Ins(1, 4, 5)P₃ response has been suggested by previous studies (Missiaen et al., 1994)). [Ca²⁺]_i elevations were expressed as a rate of [Ca²⁺]_i changes (nM/ms) and integrated to yield [Ca²⁺]_i changes over time (see Appendix for details). Best-fit analysis was performed for various assumed $n(\text{channel})$ and $n(\text{Ca}^{2+})$. The quality of the fit was quantified by the obtained F -value (Patel et al., 1976); large F -values indicate a good, small F -values a poor fit. Fig. 6, A–F, shows a typical example. To obtain mean F -values, F -values were normalized as a percentage of best fit ($= F_N$) of each experiment ($n = 13$,

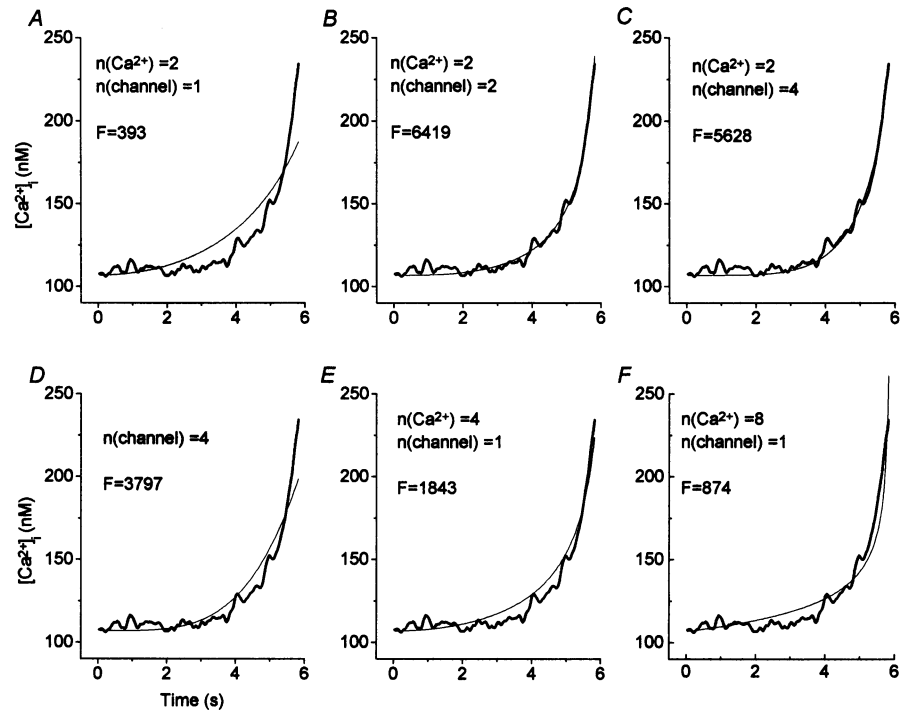
mean \pm SE). The model $n(\text{channel}) = 2$, $n(\text{Ca}^{2+}) = 2$ fitted our data best ($F_N = 79.5 \pm 6.0$). Higher cooperativity on the level of channel opening decreased the quality of the fit ($F_N = 63.0 \pm 7.0$ and $F_N = 50.0 \pm 6.0$, for $n(\text{channel}) = 4$ and 8, respectively). The model $n(\text{channel}) = 4$, no Ca²⁺ feedback, yielded the second best fit ($F_N = 64.5 \pm 10.5$). Relatively poor fitting results were obtained with models exclusively based on Ca²⁺ feedback (F_N between 37.0 ± 10.5 and 50.5 ± 9.0), even when admitting a high cooperativity on the level of the Ca²⁺ feedback (up to $n(\text{Ca}^{2+}) = 8$).

We have also taken into consideration that an activation of the Ca²⁺-ATPase might contribute to the shape of the observed Ins(1, 4, 5)P₃ concentration-response curves. Activation of the Ca²⁺-ATPase might compensate small amounts of Ca²⁺ released into the cytosol and thereby generate pseudo-cooperative Ins(1, 4, 5)P₃ dose-response curves. We have therefore evaluated the effect of the inclusion of a Ca²⁺-ATPase activity in the multiparameter curve-fitting analysis. The fitting suggested that Ca²⁺-ATPase activation by itself is not sufficient to explain a positive cooperativity when the $n(\text{channel})$ is defined as noncooperative ($n = 1$). In addition, the inclusion of a Ca²⁺-ATPase activity in the multiparameter curve fitting did not significantly modify the $n(\text{channel})$ values obtained by the best-fit analysis (results and details of the analysis not shown).

DISCUSSION

In this study, we have developed a mathematical description of the Ca²⁺ release after Ins(1, 4, 5)P₃ microperfusion through a patch-clamp pipette. Best-fit analysis of experimental data using this mathematical description suggests a very high cooperativity of the onset kinetics of Ins(1, 4, 5)P₃-induced [Ca²⁺]_i elevations. When a positive feedback of [Ca²⁺]_i on Ins(1, 4, 5)P₃-induced Ca²⁺ release was included in the mathematical description, our results

FIGURE 6 Multiparameter curve-fitting analysis of $[Ca^{2+}]_i$ elevations in response to microperfusion of $Ins(1, 4, 5)P_3$. An HL-60 granulocyte was microperfused with $10 \mu M$ $Ins(1, 4, 5)P_3$ in a Ca^{2+} -containing medium. Phases 1 and 2 (see Fig. 3 A) were used for the analysis (assumed τ 40 s). A series of Hill equations describing $Ins(1, 4, 5)P_3$ -induced Ca^{2+} release, as well as positive $[Ca^{2+}]_i$ feedback on Ca^{2+} release, are described in the Appendix. These equations were used in a best-fit procedure. The quality of the fit was analyzed, assuming various cooperativity values on the level of channel opening, $n(\text{channel})$, as well as on the level of $[Ca^{2+}]_i$ feedback, $n(Ca^{2+})$. (A–F) Fitting of a typical experiment. Best fits obtained for various values for $n(\text{channel})$ and $n(Ca^{2+})$ and the corresponding F -values are shown (note that a high F -value corresponds to a good fit). F -values were normalized (F_N) as a percentage of best fit of each experiment ($n = 13$, mean \pm SE). The values of $F_N \pm$ SE for panels A–F were, respectively, 37.0 ± 10.5 (A), 79.5 ± 6.0 (B), 63.0 ± 7.0 (C), 64.5 ± 10.5 (D), 50.5 ± 9.0 (E), and 48.5 ± 12.0 (F).



could be best fitted by a model assuming a synergy of moderately cooperative channel opening and a positive Ca^{2+} feedback.

As discussed previously (Taylor, 1992), concentration-response curves for $Ins(1, 4, 5)P_3$ -induced $[Ca^{2+}]_i$ elevations have to be analyzed with caution. They do not necessarily reflect the concentration-response of $Ins(1, 4, 5)P_3$ -induced channel opening as they may be heavily influenced by other factors, such as the onset of negative feedback mechanisms, heterogeneity of the $Ins(1, 4, 5)P_3$ -sensitivity of different cells, or heterogeneity of the $Ins(1, 4, 5)P_3$ -sensitivity of Ca^{2+} pools within one cell. Note that with respect to the cooperativity, these phenomena would tend to generate shallower concentration-response curves, i.e., they would tend to obscure a cooperativity of $Ins(1, 4, 5)P_3$ -induced Ca^{2+} release. To avoid the problem of negative feedback mechanisms, only the initial kinetics of $Ins(1, 4, 5)P_3$ -induced $[Ca^{2+}]_i$ elevations should be studied. However, even among studies with high time resolution, the results obtained so far are inconsistent: two studies found noncooperative concentration-response curves (Finch et al., 1991; Bezprozvanny et al., 1991), two studies found a moderately cooperative behavior with Hill coefficients around 2 (Iino and Endo, 1992; Champeil et al., 1989), and two studies found a highly cooperative behavior with Hill coefficients >3 (Meyer et al., 1988, 1990).

Advantages and limitations of our experimental approach

In this study we have taken advantage of the combined microfluorimetry/patch-clamp technique to analyze with a

high time resolution (20 ms) the cooperativity of $Ins(1, 4, 5)P_3$ -induced $[Ca^{2+}]_i$ elevations in single HL-60 granulocytes. $Ins(1, 4, 5)P_3$ was applied intracellularly by microperfusion through the patch pipette, and the $[Ca^{2+}]_i$ response was measured by double-emission fluorimetry. As the $Ins(1, 4, 5)P_3$ -microperfusion will generate a ramp of $Ins(1, 4, 5)P_3$ concentrations within the cytosol of the cell, the microperfusion experiments can be considered as rapid, continuous concentration-response curves. This approach has several advantages as compared to the more traditional approaches:

i) Analysis of responses in "quasi-intact" cells

As the onset of the microperfusion is identical with the onset of cellular permeabilization (i.e., break-in), one may choose conditions that allow completion of the analysis before significant outward diffusion of cytosolic components has occurred. For example, in the case of microperfusion of $10 \mu M$ $Ins(1, 4, 5)P_3$, the part of the recording that was used for analysis (i.e., phase 1 and 2 of the $Ins(1, 4, 5)P_3$ response; see Fig. 3) was obtained in less than 10 s after rupture of the plasma membrane.

ii) Analysis of responses in single cells

The affinity of the $Ins(1, 4, 5)P_3$ receptor for $Ins(1, 4, 5)P_3$ is highly regulated and varies among individual cells (Pietri et al., 1990; Joseph et al., 1989; Marshall and Taylor, 1993; Mauger et al., 1994; Champeil et al., 1989; Meyer and Stryer, 1990; Bootman et al., 1992; Oldershaw et al., 1991). If cell-to-cell variations of the affinity for $Ins(1, 4, 5)P_3$

exist, only a single-cell analysis is likely to yield meaningful values concerning the cooperativity of the response.

iii) *Precise kinetics of the increase of [Ins(1, 4, 5)P₃]_i*

Previous studies investigating the fast kinetics of the Ins(1, 4, 5)P₃ response have added Ins(1, 4, 5)P₃ to the incubation medium and applied rapid mixing techniques (Meyer et al., 1988, 1990; Champeil et al., 1989; Finch et al., 1991) or have used flash photolysis (Iino and Endo, 1992; Parker and Miledi, 1989). As the diffusion of Ins(1, 4, 5)P₃ to its site of action is not controlled in the latter systems, there always remains a considerable uncertainty as to whether the observed rapid kinetics reflect Ins(1, 4, 5)P₃ diffusion or channel opening. In contrast, in our experimental system, i) no delay of Ins(1, 4, 5)P₃ delivery to the cell exists, because a precise, equilibrated Ins(1, 4, 5)P₃ concentration is in the pipette in the cell-attached mode, and ii) the kinetics of Ins(1, 4, 5)P₃ diffusion through the tip of the patch pipette and through the cytosol are well-controlled and well-studied phenomena.

However, our experimental system has also limitations that should be noted:

i) Only the kinetics of the intracellular Ins(1, 4, 5)P₃ concentration, but not the absolute values are precisely controlled. The kinetics of microperfusion of small-molecular-weight substances, such as Ins(1, 4, 5)P₃, clearly follows a monoexponential decay (Mathias et al., 1990; Oliva et al., 1988; Pusch and Neher, 1988). However, we can only approximate the time constant for Ins(1, 4, 5)P₃ microperfusion; thus, we do not know absolute [Ins(1, 4, 5)P₃]_i values at a given time. As discussed, the assumed time constant does not influence the steepness (i.e., the Hill coefficient) of the concentration-response curves.

ii) Only the initial part of the Ins(1, 4, 5)P₃ concentration-response curve could be used for analysis. Because of the abrupt termination of Ins(1, 4, 5)P₃-induced Ca²⁺ release, approximately 5 to 10 s after the beginning of the Ins(1, 4, 5)P₃ microperfusion (see transition from phase 2 to phase 3, Fig. 3A) only the initial part of the concentration-response curve could be analyzed. This clearly led to a considerable variability of the extrapolated y_{\max} values. In contrast, as judged from the standard error, our calculated Hill coefficients were reasonably well determined by the onset of the concentration-response curve. Note that fitting the Hill equation in its nonlinear form, as done in this study, is the preferred method of obtaining Hill coefficients in the absence of a precisely determined maximum (Barlow and Blake, 1989).

iii) The concentration response was obtained by ramps of increasing Ins(1, 4, 5)P₃ concentration. Rather than adding a given Ins(1, 4, 5)P₃ concentration to one cell and measuring the response, our experiments detect a continuously increasing Ca²⁺ release in response to a continuously increasing Ins(1, 4, 5)P₃ concentration. Thus, time-dependent changes in the interaction between Ins(1, 4, 5)P₃ and its receptor may occur. Basically, there might be a time-dependent

enhancement or a time-dependent attenuation of Ins(1, 4, 5)P₃-induced Ca²⁺ release. The former corresponds to a positive cooperativity and is therefore directly related to the question studied in the manuscript. Conversely, time-dependent attenuation (e.g., due to use-dependent inactivation) potentially leads to an artificial flattening of the dose-response curve and thereby to an underestimation of the positive cooperativity of the [Ca²⁺]_i response (see v) Negative Feedback Mechanisms). Given the rapidity of our measurements, these adaptation responses will not necessarily have a major influence on the shape of the dose-response curves. This is indeed experimentally demonstrated by the observation that a slowing down of the ramp of Ins(1, 4, 5)P₃ concentrations by a factor of 5 did not change the observed Hill coefficients (Fig. 3B). Note also that the addition of a given concentration of Ins(1, 4, 5)P₃ under standard experimental conditions will also lead to a ramp of Ins(1, 4, 5)P₃ concentration, because of the relative slowness of the mixing procedure.

iv) No spatial resolution of the Ca²⁺ signal on a subcellular level was attempted. Might a spatial heterogeneity of the Ca²⁺ signal during the microperfusion of Ins(1, 4, 5)P₃ be responsible for the observed cooperativity? As an inherent feature of the microperfusion method, intracellular Ca²⁺ stores that are close to the pipette tip are exposed to a given Ins(1, 4, 5)P₃ concentration before Ca²⁺ stores that are located in distal parts of the cell. The ramp of Ins(1, 4, 5)P₃ concentrations therefore occurs earlier close to the pipette tip and later in the distal parts of the cells, leading to a flattening of the average dose-response curve of the entire cell. Thus, the lack of subcellular resolution might lead to an underestimation of the cooperativity. However, the relevance of this phenomenon depends on the relative size of a) the time constant for diffusion of Ins(1, 4, 5)P₃ within the cytosol, and b) the time constant for diffusion of Ins(1, 4, 5)P₃ from the pipette to the cytosol. If the former is much smaller than the latter, the error due to measurements of average cellular [Ca²⁺]_i elevations would be small. As an HL-60 granulocyte is very small (~5–8 μm diameter), and the cytosolic Ins(1, 4, 5)P₃ perfusion is thought to be relatively fast (20 μm²/s; Allbritton et al., 1992), the time necessary for Ins(1, 4, 5)P₃ diffusion throughout the entire cytosol is in the subsecond range. In contrast, the time constant of Ins(1, 4, 5)P₃ perfusion from the pipette into the cytosol is in the order of magnitude of 40 s, suggesting that the error due to measurements of average cellular [Ca²⁺]_i elevations was indeed small in our experiments. This was also experimentally demonstrated: when the Ins(1, 4, 5)P₃ concentration ramp was slowed down by a factor of 5 (i.e., microperfusion of 2 μM instead of 10 μM Ins(1, 4, 5)P₃; Fig. 3 B) no difference in the Hill coefficient of the Ins(1, 4, 5)P₃-induced [Ca²⁺]_i elevations was observed.

v) Onset of negative feedback mechanisms: It is clear that Ins(1, 4, 5)P₃-induced Ca²⁺ release is subject to a large number of negative feedback mechanisms, including negative feedback by [Ca²⁺]_i, receptor desensitization (Iino, 1990; Iino and Endo, 1992; Iino and Tsukioka, 1994;

Bezprozvanny et al., 1991), and decrease of the store Ca^{2+} concentration. By analyzing only the early phase of $[\text{Ca}^{2+}]_i$ elevations after $\text{Ins}(1, 4, 5)\text{P}_3$ microperfusion, we have limited the impact of the negative feedback mechanisms, but we certainly cannot exclude the possibility that they are already initiated during our time of analysis. Negative feedback mechanisms would lead to an artificial flattening of the $[\text{Ca}^{2+}]_i$ elevations in response to a ramp of $\text{Ins}(1, 4, 5)\text{P}_3$ concentration. Thus, the onset of negative feedback mechanisms might lead to an underestimation of the cooperativity of the response.

vi) The concentration of other cytosolic components changes in parallel with the InsP_3 concentration. To achieve selectively rapid changes of the cytosolic InsP_3 concentration, we used InsP_3 concentrations in the pipette that were at least 10 times higher than the concentrations we ultimately wanted to achieve within the cytosol. We therefore were able to achieve physiologically relevant changes in the cytosolic InsP_3 concentration during a time period that did not allow significant changes in the concentration of other cytosolic components.

vii) Contribution of $\text{Ins}(1, 4, 5)\text{P}_3$ metabolism to the observed cooperativity: There are two main enzymes that metabolize $\text{Ins}(1, 4, 5)\text{P}_3$: the $\text{Ins}(1, 4, 5)\text{P}_3$ -5-phosphatase and the $\text{Ins}(1, 4, 5)\text{P}_3$ -3-kinase (Connolly et al., 1985; Biden and Wollheim, 1986). It is unlikely that the $\text{Ins}(1, 4, 5)\text{P}_3$ -5-phosphatase has a relevant impact on the shape of the dose-response curve because it has a low affinity ($\sim 30 \mu\text{M}$) and, if any relevant degradation through this enzyme occurs, it should be roughly proportional to the $\text{Ins}(1, 4, 5)\text{P}_3$ concentration. In contrast, the $\text{Ins}(1, 4, 5)\text{P}_3$ -3-kinase is activated by $[\text{Ca}^{2+}]_i$ elevations in the physiological range. Thus, it is conceivable that increased $\text{Ins}(1, 4, 5)\text{P}_3$ degradation occurs as a result of the $\text{Ins}(1, 4, 5)\text{P}_3$ -induced Ca^{2+} release, leading to an artificial flattening of the dose-response curve. However, given the similar Hill values in experiments with the poorly hydrolyzable $\text{Ins}(2, 4, 5)\text{P}_3$ analog, we conclude that $\text{Ins}(1, 4, 5)\text{P}_3$ metabolism does not have a relevant influence on the observed cooperativity.

What mechanisms underlay the observed cooperativity?

The observed cooperativity of $\text{Ins}(1, 4, 5)\text{P}_3$ -induced $[\text{Ca}^{2+}]_i$ elevations might theoretically be due to a cooperativity on the level of Ca^{2+} release or to mechanisms distal to Ca^{2+} release. Mechanisms distal to Ca^{2+} release include nonlinearity of cytosolic Ca^{2+} buffering or activity of other Ca^{2+} transport mechanisms (e.g., Ca^{2+} -ATPase). We have not determined the properties of cytosolic Ca^{2+} buffering in our system; however, previous studies of granulocytes (von Tscherner et al., 1986; Nusse and Lindau, 1993) and other cell types (Zhou and Neher, 1993) did not suggest major nonlinearities in the physiological range of cytosolic Ca^{2+} buffering. In addition, pipette EGTA concentrations were very low and cells were preloaded with indo-1 to avoid

relevant changes in cytosolic Ca^{2+} buffering capacity due to EGTA and indo-1 microperfusion. With respect to activity of other Ca^{2+} transport mechanisms, we did not find (in a best-fit analysis) a significant influence of the Ca^{2+} -ATPase activity on the obtained cooperativity values (see last paragraph of the Results). Thus, although we cannot entirely exclude a contribution of factors distal to Ca^{2+} release, the observed cooperativity of $\text{Ins}(1, 4, 5)\text{P}_3$ -induced $[\text{Ca}^{2+}]_i$ elevations is most likely on the level of Ca^{2+} release. More specifically, it might be i) a cooperativity of $\text{Ins}(1, 4, 5)\text{P}_3$ binding to its receptor; ii) a cooperativity of the pore formation by four $\text{Ins}(1, 4, 5)\text{P}_3$ -receptor monomers; iii) a positive feedback by an increase of the cytosolic free Ca^{2+} concentration; or iv) a positive feedback by a decrease of the Ca^{2+} concentration within $\text{Ins}(1, 4, 5)\text{P}_3$ -sensitive Ca^{2+} stores, $[\text{Ca}^{2+}]_s$. There currently is no evidence for possibility i or iv. However, there is experimental evidence in favor of both possibilities ii (see above) and iii (Bezprozvanny et al., 1991; Iino, 1990; Parker and Ivorra, 1990; Iino and Endo, 1992; Marshall and Taylor, 1993; Iino and Tsukioka, 1994; Levitan et al., 1994).

Our results are best fitted by a model that assumes a Hill coefficient of 2 on the level of channel opening and a Hill coefficient of 2 on the level of the Ca^{2+} feedback. Thus, the steep $\text{Ins}(1, 4, 5)\text{P}_3$ concentration-response curve might be explained by the combined effect of a cooperative channel opening and a cooperative positive Ca^{2+} feedback. The model $n(\text{channel}) = 2$, $n(\text{Ca}^{2+}) = 2$ is also supported by previous studies: i) Studies with high time resolution and high concentrations of Ca^{2+} buffers yielded Hill coefficients of 2 (Iino and Endo, 1992; Iino and Tsukioka, 1994; Champeil et al., 1989); ii) patch-clamp analysis yielded a Hill coefficient of 2 for the Ca^{2+} feedback on $\text{Ins}(1, 4, 5)\text{P}_3$ -induced channel opening; and iii) $\text{Ins}(1, 4, 5)\text{P}_3$ binding to its receptor was found to be substoichiometric, raising the possibility that one $\text{Ins}(1, 4, 5)\text{P}_3$ receptor homotetramer binds only two $\text{Ins}(1, 4, 5)\text{P}_3$ molecules (Christopher et al., 1990).

However, our results would also be compatible with a cooperativity exclusively on the level of channel opening. Given recent results that challenge the importance of the positive Ca^{2+} feedback (Combettes et al., 1994), this possibility cannot be excluded. Furthermore, the possibility that there are other channel-associated mechanisms that generate cooperative curves, such as a facilitation of Ca^{2+} release by the initial drop in the store $[\text{Ca}^{2+}]_s$, should be kept in mind.

Physiological impact of the observed cooperativity

Cooperative systems allow a physiological response to occur within a small range of ligand concentrations. They are often referred to as all-or-nothing signal transducers. In the case of $\text{Ins}(1, 4, 5)\text{P}_3$ -induced Ca^{2+} release, however, the situation is more complicated. In addition to the above discussed mechanisms that increase the steepness of the

concentration-response curve, there also appear to be negative feedback mechanisms that flatten the steady-state concentration-response curve. To understand the physiological meaning of the coexistence of apparently counterbalancing mechanisms, one has to consider the dynamic range of Ins(1, 4, 5)P₃ concentrations within a cell. In HL-60 granulocytes the basal Ins(1, 4, 5)P₃ concentrations are around 250 nM, and the maximal stimulated Ins(1, 4, 5)P₃ concentrations around 2 μM (Pittet et al., 1989). Thus, taking the example of a cell with an EC₅₀ of 1 μM and a Hill coefficient of 1, Ca²⁺ release would already be constantly activated in the unstimulated cell (~15% of maximum), and the increase of Ins(1, 4, 5)P₃ concentration during cellular activation would increase this basal activity only to a limited extent (~65% of maximum). Thus the limitations of such a system for the cell would be i) a substantial basal activation of Ins(1, 4, 5)P₃-induced Ca²⁺ release and ii) the impossibility of reaching maximal Ca²⁺ release. An HL-60 granulocyte with a steep concentration-response curve for Ins(1, 4, 5)P₃-induced Ca²⁺ release ($n = 4$) clearly would go from a very low basal release (~1% of maximum) to a very high stimulated release (~95% of maximum). However, such a system would have a limited capacity for fine-tuning, and all cells would only display all-or-none responses.

Finally, an HL-60 granulocyte with a steep Ins(1, 4, 5)P₃ response and negative feedback mechanisms can maximally open its Ca²⁺ release channels in response to relatively small increases of the Ins(1, 4, 5)P₃ concentration; however, the opening of the channels will be transient because negative feedback will decrease the affinity of the Ins(1, 4, 5)P₃-receptor. A further Ca²⁺ release can be achieved, however, either through a further increase of the Ins(1, 4, 5)P₃ concentration or through regulatory changes of the affinity of the Ins(1, 4, 5)P₃ receptor.

Despite the clear physiological relevance of the cooperativity of Ins(1, 4, 5)P₃-induced Ca²⁺ release, one should keep in mind that the physiological role might not be the only explanation for the evolution of cooperative systems. In the context on his pioneering work on the cooperativity of the acetylcholine receptor, Jacques Monod stated: "Symmetrical oligomers should constitute particularly sensitive targets for molecular evolution, allowing much stronger selective pressures to operate in the random pursuit of functionally adequate structures" (Monod et al., 1965).

APPENDIX

Hill equation

The Hill equation is a nonlinear function that is often linearized to obtain simple graphical solutions. This implies a graphical linearization of the data using a Hill plot [$\log(y/(y_{\max} - y))$] as a function of $\log(x)$; the slope of the linear fit represents then the Hill coefficient. Thus, calculation of Hill coefficients by the linear graphic solution requires an accurate determination of y_{\max} (Hill, 1910; Barlow and Blake, 1989). Because of the biological properties of Ins(1, 4, 5)P₃-induced Ca²⁺ release (i.e., rapid negative feedback mechanisms), y_{\max} could not be measured in our experiments.

This problem is also frequently encountered in other biological systems and can be avoided by fitting the data with the Hill equation in its nonlinear form (A1) (Barlow and Blake, 1989). We have therefore used this approach to obtain the respective Hill coefficient. For some of our traces, however, we have used the graphical approach and obtained Hill coefficients similar to those seen with nonlinear curve fitting (data not shown).

$$y = \frac{y_{\max}}{1 + (K_d/i)^n} \quad \text{or} \quad y = \frac{y_{\max}}{1 + (EC_{50}/i)^n} \quad (\text{A1})$$

InsP₃ diffusion into the cytoplasm

The microperfusion of a substance from the pipette solution into the cytosol can be described as a single exponential decay, on the basis of both theoretical considerations (Mathias et al., 1990; Oliva et al., 1988) and experimental data (Pusch and Neher, 1988):

$$i_i = i_p * (1 - e^{-t/\tau}) \quad (\text{A2})$$

This equation was used to convert the time after break-in into cytosolic InsP₃ concentration, $[i]_i$, using various τ values (Fig. 2 and 5; see also Influence of the Assumed Time Constant on the Obtained Hill Coefficient, above).

Steepness analysis

To measure the cooperativity independently of the lag time, we have analyzed the steepness of the concentration-response curves. Using Eq. 1, we can define y_x as the response at a given concentration of InsP₃ and y_{2x} as the response for the double agonist concentration:

$$y_x = \frac{y_{\max}}{1 + (EC_{50}/x)^n}; \quad y_{2x} = \frac{y_{\max}}{1 + (EC_{50}/2x)^n}$$

The ratio of y_x and y_{2x} , i.e., the response increase for a doubling of the InsP₃ concentration, is a mathematical description of the steepness of the curve:

$$\frac{y_{2x}}{y_x} = \frac{1 + (EC_{50}/x)^n}{1 + (EC_{50}/2x)^n}$$

The InsP₃ concentration x may be expressed as a fraction of its EC₅₀:

$$x = f * EC_{50}$$

by replacing x with $f * EC_{50}$, we obtain

$$\frac{y_{2x}}{y_x} = \frac{1 + (EC_{50}/f * EC_{50})^n}{1 + (EC_{50}/2f * EC_{50})^n} \quad \text{then} \quad \frac{y_{2x}}{y_x} = \frac{1 + (1/f)^n}{1 + (1/2f)^n}$$

For InsP₃ concentrations $< EC_{50}$ the equation can be approximated as

$$\frac{y_{2x}}{y_x} \cong \frac{(1/f)^n}{(1/2f)^n} \quad \text{then} \quad \frac{y_{2x}}{y_x} \cong 2^n$$

It is therefore possible to obtain an estimate of n by calculating the base 2 logarithm of the ratio y_{2x}/y_x . For InsP₃ concentrations close to or larger than the EC₅₀, this method will lead to an underestimation, but not to an overestimation, of the Hill coefficient.

Multiparameter fitting analysis

To assess the relative role of the cooperativity of channel opening, $n(\text{channel})$, as well as the role of the positive Ca²⁺ feedback, $n(\text{Ca}^{2+})$, we described InsP₃ response and Ca²⁺ feedback as three interconnected

Hill equations:

$$y = \frac{y_{\max}}{1 + (\text{EC}_{50}/i_i)^{n(\text{channel})}} \quad (\text{HE1})$$

$$y_{\max} = \frac{y_{\max(\text{HE2})}}{1 + (\text{EC}_{50(\text{HE2})}/[\text{Ca}^{2+}]_{i(x)})^{n(\text{Ca}^{2+})}} \quad (\text{HE2})$$

$$\text{EC}_{50} = \frac{y_{\max(\text{HE3})}}{1 + (\text{EC}_{50(\text{HE3})}/[\text{Ca}^{2+}]_{i(x)})^{-n(\text{Ca}^{2+})}} \quad (\text{HE3})$$

HE1 is the same as Eq. 1 except that y_{\max} and EC_{50} are functions of HE2 and HE3, respectively. HE2 and HE3 describe the dependence of y_{\max} and EC_{50} on $[\text{Ca}^{2+}]_i$ (it has indeed been suggested that $[\text{Ca}^{2+}]_i$ decreases the EC_{50} and increases the y_{\max} of the InsP_3 response (Missiaen et al., 1994)).

HE1, HE2, and HE3 are integrated as

$$[\text{Ca}^{2+}]_{i(x+s)} = [\text{Ca}^{2+}]_{i(x)} + s * y$$

where $[\text{Ca}^{2+}]_{i(x)}$ is $[\text{Ca}^{2+}]_i$ at a given time, $[\text{Ca}^{2+}]_{i(x+s)}$ is $[\text{Ca}^{2+}]_i$ on the next sampling point, s is the sampling interval (ms), and y is the InsP_3 response derived from HE 1. As HE1 depends on HE2 and HE3, y depends on all three equations and is influenced by $n(\text{channel})$ and $n(\text{Ca}^{2+})$.

The authors would like to thank Drs. R. A. Clark and S. Rawlings for critical reading of the manuscript.

This study was funded by grants from the Swiss National Foundation (32-30161.90), the Carlos and Elsie de Reuter Foundation (Geneva), the Sandoz Foundation (Basel), the Ernst and Lucie Schmidheiny Foundation (Geneva), and the Société Académique (Geneva). J. Schrenzel was supported by a young investigators grant from the Swiss National Foundation (32-38815.93) and the Janggen Poehn Foundation (St-Gallen).

REFERENCES

- Allbritton, N. L., T. Meyer, and L. Stryer. 1992. Range of messenger action of calcium ion and inositol 1,4,5-trisphosphate. *Science*. 258: 1812–1815.
- Almers, W., and E. Neher. 1985. The Ca^{2+} signal from fura-2 loaded mast cells depends strongly on the method of dye-loading. *FEBS Lett.* 192: 13–18.
- Barlow, R., and J. F. Blake. 1989. Hill coefficients and the logistic equation. *Trends Pharmacol. Sci.* 10:440–441.
- Berridge, M. J. 1993. Inositol trisphosphate and calcium signalling. *Nature*. 361:315–325.
- Bezprozvany, I., J. Watras, and B. E. Ehrlich. 1991. Bell-shaped calcium-response curves of $\text{Ins}(1,4,5)\text{P}_3$ - and calcium-gated channel from endoplasmic reticulum of cerebellum. *Nature*. 351:751–754.
- Biden, T. J., and C. B. Wollheim. 1986. Ca^{2+} regulates the inositol Tris/tetrakisphosphate pathway in intact and broken preparations of insulin-secreting RINm5F cells. *J. Biol. Chem.* 261:11931–11934.
- Bootman, M. D., M. J. Berridge, and C. W. Taylor. 1992. All-or-nothing Ca^{2+} mobilization from the intracellular stores of single histamine-stimulated HeLa cells. *J. Physiol.* 450:163–178.
- Champeil, P., L. Combettes, B. Berthon, E. Doucet, S. Orlowski, and M. Claret. 1989. Fast kinetics of calcium release induced by *myo*-inositol trisphosphate in permeabilized rat hepatocytes. *J. Biol. Chem.* 264: 17665–17673.
- Christopher, C. C., S. Akitsugu, and S. Fleischer. 1990. Isolation and characterization of the inositol trisphosphate receptor from smooth muscle. *Proc. Natl. Acad. Sci. USA.* 87:2132–2136.
- Combettes, L., Z. Hannaert-Merah, J.-F. Coquil, C. Rousseau, M. Claret, S. Swillens, and P. Champeil. 1994. Rapid filtration studies of the effect of cytosolic Ca^{2+} on inositol 1,4,5-trisphosphate-induced $^{45}\text{Ca}^{2+}$ release from cerebellar microsomes. *J. Biol. Chem.* 269:17561–17571.
- Connolly, T. M., T. E. Bross, and P. W. Majerus. 1985. Isolation of a phosphomonoesterase from human platelets that specifically hydrolyzes the 5-phosphate of inositol 1,4,5-trisphosphate. *J. Biol. Chem.* 260: 7868–7874.
- Demaurex, N., W. Schlegel, P. Varnai, G. W. Mayr, D. P. Lew, and K. H. Krause. 1992. Regulation of Ca^{2+} influx in myeloid cells: role of plasma membrane potential, inositol phosphates, cytosolic free $[\text{Ca}^{2+}]$, and filling state of intracellular Ca^{2+} stores. *J. Clin. Invest.* 90:830–839.
- Facklam, M., P. Schoch, and W. E. Haefely. 1992. Relationship between benzodiazepine receptor occupancy and potentiation of *t*-aminobutyric acid-stimulated chloride flux in vitro of four ligands of differing intrinsic efficacies. *J. Pharmacol. Exp. Ther.* 261:76–82.
- Favre, C., D. P. Lew, and K.-H. Krause. 1994. Rapid, heparin-sensitive Ca^{2+} release following Ca^{2+} -ATPase inhibition in intact HL-60 granulocytes. *Biochem. J.* 302:155–162.
- Finch, E. A., T. J. Turner, and S. M. Goldin. 1991. Calcium as a coagonist of inositol 1,4,5-trisphosphate-induced calcium release. *Science*. 252: 443–446.
- Hamill, O. P., A. Marty, E. Neher, B. Sakman, and F. Sigworth. 1981. Improved patch clamp techniques for high-resolution current recording from cells and cell-free membrane patches. *Pflügers Arch.* 391:85–100.
- Henne, V., G. W. Mayr, B. Grabowski, B. Koppitz, and H. D. Soling. 1988. Semisynthetic derivatives of inositol 1,4,5-trisphosphate substituted at the 1-phosphate group. Effects on calcium release from permeabilized guinea-pig parotid acinar cells and comparison with binding to aldolase A. *Eur. J. Biochem.* 174:95–101.
- Hill, A. V. 1910. The possible effects of the aggregation of the molecules of haemoglobin on its dissociation curves. *Proc. Physiol. Soc.* 2:iv-vii.
- Iino, M. 1990. Biphasic Ca^{2+} dependence of inositol 1,4,5-trisphosphate-induced Ca^{2+} release in smooth muscle cells of the guinea pig taenia caeci. *J. Gen. Physiol.* 95:1103–1122.
- Iino, M., and M. Endo. 1992. Calcium-dependent immediate feedback control of inositol 1,4,5-trisphosphate-induced Ca^{2+} release. *Nature*. 360:76–78.
- Iino, M., and M. Tsukioka. 1994. Feedback control of inositol trisphosphate signalling by calcium. *Mol. Cell. Endocrinol.* 98:141–146.
- Joseph, S. K., H. L. Rice, and J. R. Williamson. 1989. The effect of external calcium and pH on inositol trisphosphate-mediated calcium release from cerebellum microsomal fractions. *Biochem. J.* 258: 261–265.
- Levitan, I., R. Payne, B. V. L. Potter, and P. Hillman. 1994. Facilitation of the responses to injections of inositol 1,4,5-trisphosphate analogs in *Limulus* ventral photoreceptors. *Biophys. J.* 67:1161–1172.
- Marshall, I. C. B., and C. W. Taylor. 1993. Biphasic effects of cytosolic Ca^{2+} on $\text{Ins}(1,4,5)\text{P}_3$ -stimulated Ca^{2+} mobilization in hepatocytes. *J. Biol. Chem.* 268:13214–13220.
- Mathias, R. T., I. S. Cohen, and C. Oliva. 1990. Limitations of the whole cell patch clamp technique in the control of intracellular concentrations. *Biophys. J.* 58:759–770.
- Mauger, J.-P., J.-P. Lièvreumont, F. Piétri-Rouxel, M. Hilly, and J.-F. Coquil. 1994. The inositol 1,4,5-trisphosphate receptor: kinetic properties and regulation. *Mol. Cell. Endocrinol.* 98:133–139.
- Meyer, T., D. Holowka, and L. Stryer. 1988. Highly cooperative opening of calcium channels by inositol 1,4,5-trisphosphate. *Science*. 240: 653–656.
- Meyer, T., and L. Stryer. 1990. Transient calcium release induced by successive increments of inositol 1,4,5-trisphosphate. *Proc. Natl. Acad. Sci. USA.* 87:3841–3845.
- Meyer, T., T. Wensel, and L. Stryer. 1990. Kinetics of calcium channel opening by inositol 1,4,5-trisphosphate. *Biochemistry*. 29:32–37.
- Missiaen, L., H. De Smedt, J. B. Parys, and R. Casteels. 1994. Co-activation of inositol trisphosphate-induced Ca^{2+} release by cytosolic Ca^{2+} is loading-dependent. *J. Biol. Chem.* 269:7238–7242.
- Monod, J., J. Wyman, and J.-P. Changeux. 1965. On the nature of allosteric transitions: a plausible model. *J. Mol. Biol.* 12:88–118.
- Nunn, D. L., and C. W. Taylor. 1990. Liver inositol 1,4,5-trisphosphate-binding sites are the Ca^{2+} -mobilizing receptors. *Biochem. J.* 270: 227–232.

- Nuesse, O., and M. Lindau. 1993. The calcium signal in human neutrophils and its relation to exocytosis investigated by patch clamp capacitance and Fura-2 measurements. *Cell Calcium*. 14:255–269.
- Oldershaw, K. A., D. L. Nunn, and C. W. Taylor. 1991. Quantal Ca²⁺ mobilization stimulated by inositol 1,4,5-trisphosphate in permeabilized hepatocytes. *Biochem. J.* 278:705–708.
- Oliva, C., I. S. Cohen, and R. T. Mathias. 1988. Calculation of time constants for intracellular diffusion in whole cell patch clamp configuration. *Biophys. J.* 54:791–799.
- Parker, I., and I. Ivorra. 1990. Inhibition by Ca²⁺ of inositol trisphosphate-mediated Ca²⁺ liberation: a possible mechanism for oscillatory release of Ca²⁺. *Proc. Natl. Acad. Sci. USA.* 87:260–264.
- Parker, I., and R. Miledi. 1989. Nonlinearity and facilitation in phosphoinositide signaling studied by the use of caged inositol trisphosphate in *Xenopus* oocytes. *J. Neurosci.* 9:4068–4077.
- Patel, J. K., C. H. Kapadia, and D. B. Owen. 1976. *Handbook of Statistical Distributions*. Vol. 20. M. Dekker, New York.
- Pietri, F., M. Hilly, and J. P. Mauger. 1990. Calcium mediates the interconversion between two states of the liver inositol 1,4,5-trisphosphate receptor. *J. Biol. Chem.* 265:17478–17485.
- Pittet, D., W. Schlegel, D. P. Lew, A. Monod, and G. W. Mayr. 1989. Mass changes in inositol tetrakis- and pentakisphosphate isomers induced by chemotactic peptide stimulation in HL-60 cells. *J. Biol. Chem.* 264:18489–18493.
- Pusch, M., and E. Neher. 1988. Rates of diffusional exchange between small cells and a measuring patch pipette. *Pflügers Arch.* 411:204–211.
- Spaet, A., P. G. Bradford, J. S. McKinney, R. P. Rubin, and J. W. J. Putney. 1986. A saturable receptor for ³²P-inositol-1,4,5-trisphosphate in hepatocytes and neutrophils. *Nature.* 319:514–516.
- Taylor, C. W. 1992. Kinetics of inositol 1,4,5-trisphosphate-stimulated Ca²⁺ mobilization. In *Advances in Second Messenger and Phosphoprotein Research*, Vol. 26. J. W. Putney, editor. Raven Press, New York. 109–142.
- Van Delden, C., C. Favre, A. Spat, E. Cerny, K. H. Krause, and D. P. Lew. 1992a. Purification of an inositol 1,4,5-trisphosphate-binding calreticulin-containing intracellular compartment of HL-60 cells. *Biochemical Journal* 281, 651–656.
- Van Delden, C., M. Foti, D. P. Lew, and K. H. Krause. 1993. Ca²⁺ and Mg²⁺ regulation of Ins(1, 4, 5)P₃ binding in myeloid cells. *J. Biol. Chem.* 268:12443–12448.
- Van Delden, C., M. E. E. Jaconi, D. Pittet, N. Demaurex, K.-H. Krause, and D. P. Lew. 1992b. Calcium translocation in signal transduction. In *Cellular and Molecular Mechanisms of Inflammation*, Vol. 3. Academic Press, New York. 115–151.
- Varnai, P., N. Demaurex, M. E. E. Jaconi, W. Schlegel, D. P. Lew, and K. H. Krause. 1993. Highly cooperative Ca²⁺ activation of intermediate conductance K⁺ channels in HL-60 granulocytes. *J. Physiol.* 472:373–390.
- Von Tschärner, V., D. A. Deranleau, and M. Baggiolini. 1986. Calcium fluxes and calcium buffering in human neutrophils. *J. Biol. Chem.* 261:10163–10168.
- Worley, P. F., J. M. Baraban, and S. H. Snyder. 1989. Inositol 1,4,5-trisphosphate receptor binding: autoradiographic localization in rat brain. *J. Neurosci.* 9:339–346.
- Zhou, Z., and E. Neher. 1993. Mobile and immobile calcium buffers in bovine adrenal chromaffin cells. *J. Physiol.* 469:245–273.